Ligand Binding inside the Cavities of Lacunar and Saddle-Shaped Cyclidene Complexes: Molecular Mechanics and Molecular Dynamics Studies

Elena V. Rybak-Akimova*,†,‡ and Krzysztof Kuczera*,†,§

Departments of Chemistry and Biochemistry, University of Kansas, Lawrence, Kansas 66045, and Tufts University, Department of Chemistry, Medford, Massachusetts 02155

Received June 24, 1999

Cobalt(II) complexes with tetradentate macrocyclic cyclidene ligands are known to coordinate one additional axial base molecule, leaving the sixth vacant coordination site at the metal ion available for small ligand (e.g., O_2) binding. Molecular mechanics and molecular dynamics simulations provide a microscopic view of 1-methylimidazole (MeIm) binding within the cavities of several lacunar (bridged) and saddle-shaped (unbridged) cyclidenes and uncover the roles of the bridges and the walls of the clefts in steric protection of the cobalt(II) coordination site. Short bridges (C3 and C6) prevent inside-the-cavity MeIm binding because of severe ligand distortions leading to high-energy penalties (58 and 25 kcal/mol, respectively), while long bridges (C8 and C12) flip away from the MeIm binding site, allowing for penalty-free MeIm inclusion. In the unbridged saddle-shaped complex, there is no energy difference between inside- and outside-the-cavity MeIm binding. The preferential existence of the coordinatively unsaturated, five-coordinate species Co(unbrCyc)$(MeIm)^{2+}$ should therefore be explained by electronic, rather than steric, factors. Molecular dynamics and free energy simulations reveal the presence of a weak (ca. 4 kcal/mol in the gas phase and ca. 2 kcal/mol in methanol solution) noncovalent MeIm binding site at the entrance of the cleft of cobalt(II) unbridged cyclidene, at a distance of about 4 Å from the metal ion. The macrocycle geometry remains undistorted at such large Co−N(MeIm) separations, while the cavity opens up by 0.9 Å upon covalent MeIm binding (Co−N(MeIm) distance of 2 Å). An increase in macrocycle strain energy upon MeIm inclusion is compensated by favorable nonbonded interactions between the incoming base and the walls of the unbridged cyclidene.

Introduction

Transition metal complexes having a protected vacant coordination site at the metal ion are important for small molecule binding and activation.[1−10] These molecules are used, for example, as reversible dioxygen carriers[1,2] and redox catalysts.[8] Steric protection of a vacant site serves several purposes, among them, (1) prevention of autoxidation reactions that proceed via peroxo-bridge formation, (2) discrimination between relatively large solvent and/or base molecules present in the reaction media, and small dioxygen molecules (ideally, only the latter ones will find an access to the metal ion), (3) possibly, shielding of the coordination site from uncoordinated solvent molecules, thus facilitating small ligand binding.[11] To create sterically protected sites at the metal ion, different approaches have been used, such as the introduction of bulky substituents in the vicinity of the metal ion[1,3,4] and the building of superstructures around the metal ion vacant site.[1,2] The latter approach has been widely used for the porphyrins[1] and also proved to be very successful for non-porphyrin ligands.[2] Among the non-porphyrin lacunar complexes, cyclidenes have been extensively studied.[2] The cobalt(II) and iron(II) cyclidenes reversibly bind dioxygen;[2,12−14] the dioxygen adducts formed can be used for oxygenation of other substrates.[15]

Lacunar cyclidene complexes of cobalt(II) were found to exist in solutions as five-coordinate species, with only one axial base or solvent molecule bound to the cobalt(II) macrocycle.[16] In principle, both steric and electronic factors might be responsible for the preferential formation of five-coordinate low-spin cobalt(II) species. For the bridged (lacunar) cyclidenes, this has been traditionally attributed to the protection of the sixth coordination site by the lacuna.[2,14,16] The relative role of steric and electronic factors in protecting the sixth Co(II) coordination site in bridged and unbridged cyclidenes has not, however, been studied. It is also unclear whether the steric protection in lacunar complexes is provided by the "roof" of the cavity (the bridge) or by the "walls" of the cavity (which are produced by the unsaturated

† Department of Chemistry, University of Kansas.
‡ Tufts University.
§ Department of Biochemistry, University of Kansas.

(1) Momenteau, M.; Reed, C. A. *Chem. Rev.* **1994**, *94*, 659.
(2) Busch, D. H.; Alcock, N. W. *Chem. Rev.* **1994**, *94*, 585.
(3) Feig, A. L.; Lippard, S. J. *Chem. Rev.* **1994**, *94*, 759.
(4) Que, L., Jr. *J. Chem. Soc., Dalton Trans.* **1997**, 3933.
(5) Hayashi, Y.; Suzuki, M.; Uehara, A.; Mizutani, Y.; Kitagawa, T. *Chem. Lett.* **1992**, 91.
(6) Uozumi, K.; Hayashi, Y.; Suzuki, M.; Uehara, A. *Chem. Lett.* **1993**, 963.
(7) Tolman, W. B. *Acc. Chem. Res.* **1997**, *30*, 227.
(8) Suslick, K. S.; van Deusen-Jeffries, S. *Compr. Supramol. Chem.* **1996**, *5*, 141.
(9) Schrock, R. R. *Acc. Chem. Res.* **1997**, *30*, 9.
(10) Cummins, C. C. *Chem. Commun.* **1998**, 1777.
(11) Collman, J. P.; Brauman, J. I.; Iverson, B. L.; Sessler, J. L.; Morris, R. M.; Gibson, Q. H. *J. Am. Chem. Soc.* **1983**, *105*, 3052.
(12) Stevens, J. C.; Busch, D. H. *J. Am. Chem. Soc.* **1980**, *102*, 3285.
(13) Herron, N.; Busch, D. H. *J. Am. Chem. Soc.* **1981**, *103*, 1236.
(14) Busch, D. H.; Jackson, P. J.; Kojima, M.; Chmielewski, P.; Matsumoto, N.; Stevens, J. C.; Wu, W.; Nosco, D.; Herron, N.; Ye, N.; Warburton, P. R.; Masarwa, M.; Stephenson, N. A.; Christoph, G.; Alcock, N. W. *Inorg. Chem.* **1994**, *33*, 910.
(15) Deng, Y.; Busch, D. H. *Inorg. Chem.* **1995**, *34*, 6380.
(16) Stevens, J. C.; Jackson, P. J.; Schammel, W. P.; Christoph, G. G.; Busch, D. H. *J. Am. Chem. Soc.* **1980**, *102*, 3283.

10.1021/ic990738l CCC: $19.00
Published on Web 05/24/2000

six-membered chelate rings in these U-shaped macrocycles). In the case of small molecule (O_2) binding, the role of the "walls" seems to be significant. It has been demonstrated that dioxygen affinity of bridged Co(II) cyclidenes is determined by the length of the bridge, which, in turn, correlates with the cavity width.[2,14] Consequently, the distance between the "walls" is an important factor in the dioxygen binding; the bridges of different length span the "walls" of the cavity to a different extent. The cavity width is reflected primarily in the O_2 binding rates (the greater the opening of the cavity, the more orientations of the O_2 molecule lead to its coordination).[17] Another effect, steric interaction between the bridge (the "roof") and the coordinated O_2 molecule, has also been identified in some cases. This leads to the decrease of dioxygen affinities, sometimes by several orders of magnitude.[18] The O_2−bridge interaction is significant for short bridges, or for bridges in "straight" ("zigzag") conformations, which cannot fold out of the metal center;[14,18] these "straight-over-the-cavity" conformations of the bridges cause fast Co−O_2 dissociation rates.[18]

There is some direct experimental evidence for the restricted solvent/ligand access to the metal site in bridged and unbridged saddle-shaped cyclidenes.[2] It is difficult to clearly distinguish experimentally the roles of the walls and the roof of the cyclidene molecules in shielding the central metal ion because introducing bridges of different length and structure in the cyclidenes (the roof) affects the cavity width (the distance between the walls). We present here the computational analysis of the role of different steric factors in the protection of the sixth cobalt(II) coordination site from the binding of solvent or axial base molecules. A comparison between an unbridged cyclidene and complexes having polymethylene bridges of different length (Figure 1) allows us to uncover the functions of the "walls" and the "roof" of the lacuna. The 16-membered cyclidene macrocycles retain their saddle-shaped conformation even in the absence of the bridge[19] (Figure 2a), and the cavity width is comparable to that of the C6-bridged complexes[2,14] (Figure 2b). The unbridged cobalt(II) cyclidene binds only one solvent (acetonitrile) or base (1-methylimidazole) molecule in solution,[15,20] a behavior analogous to its lacular (bridged) counterparts.[21] Consequently, the presence of the bridge in the ligand superstructure is not critical for the preferential existence of the five-coordinate species in solutions of cobalt(II) cyclidenes.

Molecular modeling studies proved to be useful in describing the microscopic solvent structure in the vicinity of cobalt(II) cyclidene complexes of various molecular shapes.[22] In this work we provide a microscopic description of 1-methylimidazole (MeIm) binding to several cyclidenes in a vacuum and in the presence of the solvent (methanol), using molecular mechanics and molecular dynamics simulations. A quantitative description of "steric effects" in ligand binding within the cavities of various

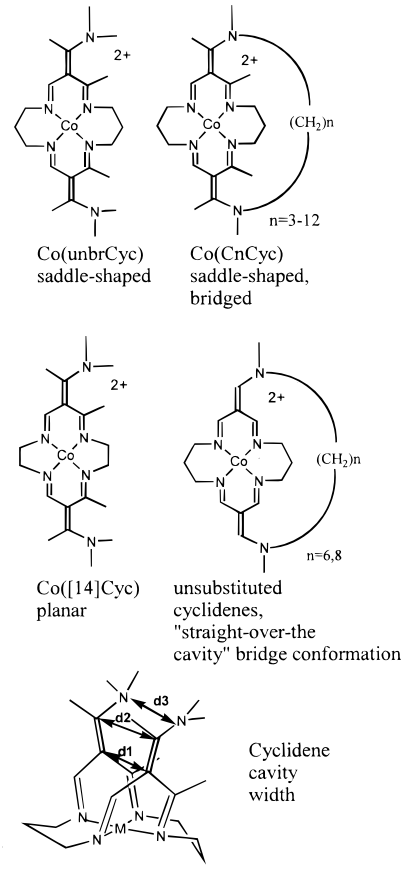

Figure 1. Cyclidene complexes.

constrained cyclidenes is the major focus of this research. The details of molecular structures, fluctuations, and energetics obtained from modeling are employed to interpret the available experimental data and to extend our understanding of the phenomena under study. The methods developed here allow for prediction of the guest binding properties of the sterically constrained cyclidene hosts. Our molecular modeling studies include (1) energy minimization for a series of bridged and unbridged complexes with 1-methylimidazole (MeIm) inside or outside the cavity, (2) construction of an adiabatic energy profile for MeIm approaching the Co(II) center in the unbridged cyclidene, (3) molecular dynamics simulations in methanol for the systems containing an unbridged Co(II) complex and MeIm, and (4) conformational free energy simulations along the Co−N(MeIm) reaction coordinate.

Methods

Molecular Mechanics Calculations. Molecular mechanics calculations were carried out with the MM2 force field implemented in CAChe Worksystem, version 3.6 (CAChe Scientific, Inc.), and the CHARMM all-atom force field[23,24] (CHARMM, versions 22, 24, and 25[25]). The modifications of the MM2/MMP2 force field, which are necessary for adequate modeling of the cyclidene geometries, have been described

(17) Rybak-Akimova, E. V.; Marek, K.; Masarwa, M.; Busch, D. H. *Inorg. Chim. Acta* **1998**, *270*, 151.
(18) Kolchinski, A. G.; Korybut-Daszkiewicz, B.; Rybak-Akimova, E. V.; Busch, D. H.; Alcock, N. W.; Clase, H. J. *J. Am. Chem. Soc.* **1997**, *119*, 4160.
(19) Alcock, N. W.; Lin, W.-K.; Jircitano, A.; Mokren, J. D.; Corfield, P. W. R.; Johnson, G.; Novotnak, G.; Cairns, C.; Busch, D. H. *Inorg. Chem.* **1987**, *26*, 440.
(20) Deng, Y. Dioxygen binding properties of the cobalt(II) cyclidene complexes and their catalytic oxygenation reactions. Ph.D. Thesis, Ohio State University, Columbus, OH, 1991.
(21) Herron, N.; Zimmer, L. L.; Grzybowski, J. J.; Olszanski, D. J.; Jackels, S. C.; Callahan, R. W.; Cameron, J. H.; Christoph, G. G.; Busch, D. H. *J. Am. Chem. Soc.* **1983**, *105*, 6585.
(22) Rybak-Akimova, E. V.; Kuczera, K.; Jas, G. S.; Deng, Y.; Busch, D. H. *Inorg. Chem.* **1999**, *38*, 3423−3434.
(23) MacKerrel, A. D., Jr.; Wiorkiewicz-Kuczera, J.; Karplus, M. *J. Am. Chem. Soc.* **1995**, *117*, 11946.
(24) MacKerrel, A. D., Jr.; Bashford, D.; Bellott, M.; Dunbrack, R. L., Jr.; Evanseck, J. D.; Field, M. J.; Fischer, S.; Gao, J.; Guo, H.; Ha, S.; Joseph-McCarthy, D.; Kuchnir, L.; Kuczera, K.; Lau, F. T. K.; Mattos, C.; Michnik, S.; Ngo, T.; Nguyen, D. T.; Prodhom, B.; Reiher, W. E., III.; Roux, B.; Schlenkrich, M.; Smith, J. C.; Stote, R.; Straub, J.; Watanabe, M.; Wiorkiewicz-Kuczera, J.; Yin, D.; Karplus, M. *J. Phys. Chem. B* **1998**, *102*, 3586.
(25) Brooks, B. R.; Bruccoleri, R. E.; Olafson, B. D.; States, D. J.; Swaminathan, S.; Karplus, M. *J. Comput. Chem.* **1983**, *4*, 187.

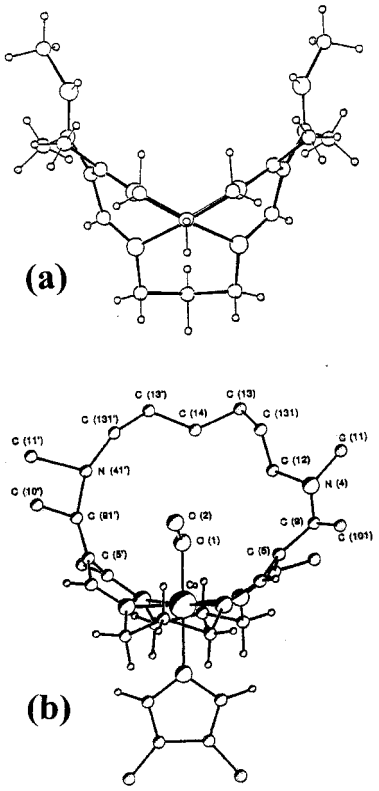

Figure 2. X-ray structures of 16-membered cyclidene complexes: (a) unbridged saddle-shaped cyclidene, Cu(H_2MeMe[16]Cyc), reproduced with permission from ref 19; (b) dioxygen adduct with C6-bridged lacunar cyclidene, [Co(C6)MeMe[16]Cyc](MeIm)(O_2). Reproduced with permission from ref 2.

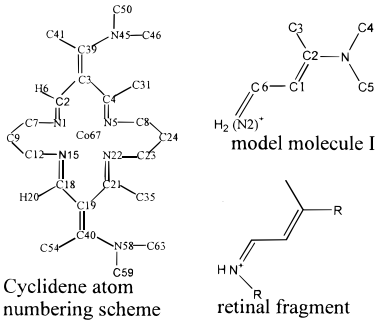

Figure 3. Cyclidene framework and model molecules used in ab initio vibrational frequency fitting procedure (CHARMM parametrization for cyclidenes).

previously;[26] the corresponding force field parameters were entered in CAChe from the menu, and the editing of the resulting text file was required to incorporate the bond dipoles. Visualization of the CHARMM calculations was done with QUANTA/CHARMm package (MSI).

Parametrization of the CHARMM force field required more extensive calculations. Several new atom types for the cyclidene macrocycles were introduced: NSB, a Schiff base nitrogen (N1, N5, N15, and N22); CET, a Schiff base carbon (C2, C4, C12, and C21); CPHM, sp^2 carbon in the conjugated part of the molecule (C3, C39, C19, and C40); HI, a Schiff base hydrogen (H6 and H20); NR1M, nitrogen atom at the periphery of the macrocycle (N45 and N58); and MCO, low-spin Co(II) in the cyclidene macrocycle (Co67) (Figure 3). The parameters developed for retinal[27−29] were used as a starting point for the Schiff base fragment of the molecule; those were refined in the subsequent ab initio calculations for model molecule **I** (Figure 3). The model molecule was chosen, among several candidates, to reproduce the bond order (and the bond lengths) at the periphery of the cobalt(II) cyclidenes. The correspondence between bond lengths obtained in ab initio geometry optimization for the model (Gaussian 92, HF/6-31G* theoretical level) and the average bond lengths found from X-ray crystallographic data for cyclidene complexes is shown in Table 1. Regardless of the initial geometry and the symmetry of the **Z** matrix, the optimized model molecule invariably had a symmetry plane. This symmetry (C_s) was imposed in the subsequent calculations of vibrational frequencies.

Table 1. Bond Lengths Found for the Cyclidene Framework and Calculated for the Model Molecule **I** (Figure 3)

cyclidenes (X-ray data)[a]		model molecule **I** (ab initio)	
bond	bond length, Å	bond	bond length, Å
N1−C2	1.28−1.30	N2−C6	1.32
C2−C3	1.42−1.44	C6−C1	1.37
C3−C39	1.41−1.43	C1−C2	1.41
C39−C41	1.49	C2−C3	1.51
C39−N45	1.32	C2−N	1.31
N45−C50	1.48	N−C4	1.48

[a] References 2 and 14 and publications cited therein.

An attempt has been made to calculate the rotational barriers about the C═C and C−N bonds in the model molecule. The energy values with the corresponding dihedral angle constrained at 0°, 30°, 60°, 90°, 120°, 150°, and 180° have been calculated (HF/6-31G* level), and the barriers were found to be equal to 15.2 and 23.2 kcal/mol, respectively. As expected from the symmetry considerations, the energies of the cis and trans isomers (0° and 180°) were the same for the C−N bond and differed by 5 kcal/mol for the C═C bond (the lower energy isomer is depicted in Figure 3). Obviously, the theoretical level used for rotational barrier calculations was insufficient for the rotations about bonds with an order higher than 1,[30−32] and the results reported here must be overestimated. NMR measurements of rotational barriers about the C−N bond in conjugated molecules (derivatives of 4-(dimethylamino)pyridine coordinated to osmium) provided the values of 13−14 kcal/mol.[33] For comparison, an experimental value of 65 kcal/mol has been reported, from thermal activation measurements, for this rotational barrier in ethylene.[34]

Since the calculations of torsional barriers for cyclidenes and their models proved to be unreliable, the vibrational frequency fitting method was used to obtain force field parameters. The CHARMM force field parameters for the introduced atom types were altered to fit ab initio vibrational frequencies of model molecule **I** (Figure 3). All ab initio frequencies were scaled by 0.9 to correct for systematic errors. Normal mode analysis of model molecule **I** was done using the MOLVIB module of CHARMM. Root-mean-square deviations between vibrational frequencies calculated in CHARMM with new parameters and scaled ab initio frequencies are 22 cm^{-1} for torsional parameters and 40 cm^{-1} for bond/angle parameters. These are suitable for the purpose of this research ("chemical accuracy"[35]). The parameters for methyl and methylene groups were not modified in this study. The values of torsional force constants are now in better agreement with experimental estimates; e.g., the force constant of 3.1 kcal/mol was obtained for rotations about the CPHM−NR1M bond (C39−N45 and C40−N58), giving a value of $4 \times 3.1 = 12.4$ kcal/mol for this "purely torsional" barrier. This value compares well with NMR data for the derivatives of 4-(dimethylamino)pyridine coordinated to osmium mentioned above (13−14 kcal/mol[33]).

(26) Lin, W.-K.; Alcock, N. W.; Busch, D. H. *J. Am. Chem. Soc.* **1991**, *113*, 7603.
(27) Nina, M.; Roux, B.; Smith, J. C. *Biophys. J.* **1995**, *68*, 25.
(28) Logunov, I.; Schulten, K. *J. Am. Chem. Soc.* **1996**, *118*, 9727.
(29) Hermone, A.; Kuczera, K. *Biochemistry* **1998**, *37*, 2843.
(30) Head-Gordon, M.; Pople, J. A. *J. Phys. Chem.* **1993**, *97*, 1147.
(31) Borrmann, A.; Jones, R. O. *Chem. Phys. Lett.* **1996**, *252*, 1.
(32) Sebastian, R.; Wallace, R. *Chem. Phys. Lett.* **1991**, *177*, 404.
(33) Djukic, J.-P.; Young, V. G., Jr.; Woo, L. K. *Organometallics* **1994**, *13*, 3995.
(34) Douglas, J. E.; Rabinovitch, B. S.; Looney, F. S. *J. Chem. Phys.* **1955**, *23*, 315.
(35) Allinger, N. L.; Yuh, Y. H.; Lii, J.-H. *J. Am. Chem. Soc.* **1989**, *111*, 8852.

Table 2. Cavity Width in Cyclidenes Spanned by Bridges of Different Length (Figures 1−3)

	d_1 (C3−C19), Å		d_2 (C39−C40), Å		d_3 (N45−N58), Å	
	X-ray data	optimized structure	X-ray data	optimized structure	X-ray data	optimized structure
Co(C3Cyc)	4.90[a]	4.71	5.76[a]	5.69	4.92[a]	4.99
Co(C6Cyc)	5.29[b]	5.30	6.63[b]	6.66	6.75[b]	6.85
Co(C8Cyc)	5.84[c]	5.75	7.75[c]	7.54	7.82[c]	7.94
Co(C12Cyc)	5.22[d]	5.32	6.64[d]	6.70	6.27[d]	6.37

[a] Alcock, N. W.; Lin, W. K.; Cairns, C.; Pike, G. A.; Busch, D. H. *J. Am. Chem. Soc.* **1989**, *111*, 6630 (data for copper(II) complex). [b] Reference 16. [c] Alcock, N. W.; Lin, W. K.; Cairns, C.; Pike, G. A.; Busch, D. H. *J. Am. Chem. Soc.* **1989**, *111*, 6630 (data for copper(II) complex). [d] Alcock, N. W.; Lin, W. K.; Cairns, C.; Pike, G. A.; Busch, D. H. *J. Am. Chem. Soc.* **1989**, *111*, 6630 (data for nickel(II) complex).

The parameters for the Co(II) coordination sphere were similar to those used in the MM2/MMP2 parameter set developed earlier.[26] Two other reference sets were used to adjust them: the CHARMM parameters for iron(II) porphyrins[36,37] and the CHARMM/MMX parameters for cobalt(II) macrocyclic amines.[38] The parameters for cobalt(II) coordination sphere were adjusted to fit the geometry of the Co(II) cyclidenes known from X-ray analysis[2] (C3-, C6-, C8-, and C12-bridged cyclidenes). Some adjustments of the r_0 and θ_0 were also done to fit the cyclidene geometry. The complete parameter list is given in Table 2 of Supporting Information.

Atomic charges for the unbridged Co(II) macrocycle, 1-methylimidazole (MeIm), and the five-coordinate complex Co(unbrCyc)(MeIm)$^{2+}$ were obtained from ZINDO calculations[39−41] (as implemented in the CAChe worksystem, SCF/UHF approximation for the doublet ground state) with Mulliken population analysis. Geometry optimization for the macrocyclic complexes did not converge; consequently, the results obtained for the X-ray structures, or for the structures optimized in MM2, were used for single-point energy calculations. Charge distributions for the four- and five-coordinated macrocyclic complexes were very similar to each other; the charges on the coordinated and noncoordinated MeIm also did not differ significantly. The charges for the four-coordinate complex and for the free 1-methylimidazole were smoothed and used in all molecular mechanics calculations. No charge scaling was possible because the Co(II) macrocycle is not a neutral species. Atomic charges for methylene groups in the bridges were standard for QUANTA/CHARMm. All charges are given in the topology list (Table 1 of Supporting Information).

Lennard-Jones parameters for the new atom types were transferred from the chemically related atom types existing in CHARMM.

The unique labeling problem[42] was overcome by deleting two undesirable angle terms (N−Co−N = 180°) from the topology file. The CHARMM principle of constructing the molecules from different "blocks" (residues and segments) by linking them together was very helpful in the building of multicomponent macrocyclic complexes. In our case, Co(unbrCyc) represented one fragment, methylimidazole represented the other fragment, and the bridge represented still another fragment (Table 1 of Supporting Information).

The acceptable quality of the developed cyclidene CHARMM force field has been confirmed by molecular mechanics calculations (energy minimization) on a series of complexes. The cyclidene geometry is known to be very sensitive to variations in the ligand structure. The following features of the X-ray crystal structures of the cyclidenes were qualitatively and quantitatively reproduced in our calculations: (1) the bridge-length-dependent variations in the cavity width for 16-membered macrocycles (C3-, C6-, C8-, and C12-bridged cyclidenes were used in the training set; the cavity width of the C5-bridged complex has also been calculated) (Table 2); (2) the substantially different conformations of the C6 bridge in the unsubstituted (R^3═R^4═H) and methyl-substituted cyclidenes;[18] (3) the saddle-shaped conformation of the 16-membered unbridged cyclidene and the "open", flat conformation of the 14-membered unbridged cyclidenes.[43] In the case of C6Cyc, an X-ray structure of the cobalt(II) complex is available,[16] thus making possible a direct comparison between crystallographic data and an optimized geometry for the complex Co(C6Cyc). The root-mean-square deviation in atomic positions is 0.086 Å, deviations in bond lengths are within 0.03 Å, and deviations in bond angles are within 2° (in most cases, deviations are actually much smaller). The same deviations in bond lengths and angles were obtained for the organic parts of other optimized cobalt(II) cyclidenes (derivatives of C3Cyc, C8Cyc, and C12Cyc), where X-ray data for Cu(II) or Ni(II) (but not Co(II)) complexes were reported.[2,44] It is also important for the force field to have a balance between the different terms, such as internal deformation and nonbonded interactions. On the basis of the results (see Table 3), this balance has been accomplished in the cyclidene force field developed here, since no single term dominates the calculated energetic effects.

Although the quality of the cyclidene force field developed and used in this work is clearly acceptable for the purpose of this research, it should be noted that this cyclidene force field is oversimplfied and based on many approximations (use of model compounds, transfer of parameters from similar fragments, ZINDO/Mulliken calculations of charges, use of vibrational spectra to fit torsional barriers). The structural parameters (bond lengths and angles) were better refined to fit experimental data specific for cyclidenes than the energetic parameters (deformation force constants, charges, van der Waals radii). Thus, we expect our models to reliably predict cyclidene system structures. The energetic results will be less reliable and should be used to qualitatively guide our understanding of the studied effects.

Energy minimization in CHARMM was performed, using the adopted basis Newton−Raphson algorithm; in MM2, the conjugate gradient or Newton−Raphson algorithms were applied. In energy calculations, an atom-based 12.0 Å nonbonded cutoff distance was employed, with a switching function between 10.0 and 12.0 Å for van der Waals terms and a shift function at 12.0 Å for electrostatics to eliminate discontinuities due to cutoff.[25] Full nonbonded interactions were calculated for all atoms separated by three or more chemical bonds. The initial geometries of the macrocycles were taken from the X-ray structural data;[2] the methylimidazole ligand bound outside the cavity was positioned as in [Co(C6Cyc)(MeIm)(O_2)]$^{2+}$.[14]

Adiabatic Energy Profile for MeIm Translation into the Macrocyclic Cleft of Co(unbrCyc). The adiabatic translational profile for MeIm entering the cavity of Co(unbrCyc) was obtained from a series of potential energy minimizations with fixed values of the Co−N(MeIm) distance. The chemical bond between Co and N(MeIm) atoms has been deleted from the topology file for these calculations. The internal coordinate (the Co−N(MeIm) distance) was constrained using a recently developed holonomic constraints algorithm.[45]

Molecular Dynamics Simulations Protocol. Standard CHARMM force field parameters and atomic charges[23,24] developed for serine and threonine side chains were used to model the potential energy function for the solvent (methanol) molecules. These parameters provide a model of liquid methanol in excellent agreement with experimental observations (calculated density of 0.79 g/cm^3 and ΔH_{vap} = 35.4 kJ/mol).[46]

Molecular dynamics simulations for Co([16]Cyc)−MeIm were performed in methanol solutions. Two independent simulations were run starting from different initial geometries (with MeIm inside the cavity and MeIm outside the cavity). For the liquid systems, the

(36) Kuczera, K.; Kuriyan, J.; Karplus, M. *J. Mol. Biol.* **1990**, *213*, 351.
(37) Petrich, J. W.; Lambry, J.-C.; Kuczera, K.; Karplus, M.; Poyart, C.; Martin, J.-L. *Biochemistry* **1991**, *30*, 3975.
(38) Gao, Y.-D.; Lipkowitz, K.; Schultz, F. A. *J. Am. Chem. Soc.* **1995**, *117*, 11932.
(39) Ridley, J. E.; Zerner, M. C. *Theor. Chim. Acta* **1976**, *42*, 223.
(40) Bacon, A. D.; Zerner, M. C. *Theor. Chim. Acta* **1979**, *53*, 21.
(41) Zerner, M. C.; Loew, G. H.; Kirchner, R. F.; Mueller-Westerhoff, U. T. *J. Am. Chem. Soc.* **1980**, *102*, 589.
(42) Zimmer, M. *Chem. Rev.* **1995**, *95*, 2629.
(43) Chen, J.; Ye, N.; Alcock, N. W.; Busch, D. H. *Inorg. Chem.* **1993**, *32*, 904.
(44) Alcock, N. W.; Lin, W. K.; Cairns, C.; Pike, G. A.; Busch, D. H. *J. Am. Chem. Soc.* **1989**, *111*, 6630.
(45) Kuczera, K. *J. Comput. Chem.* **1996**, *17*, 1726.
(46) Jas, G. S.; Kuczera, K. Unpublished results.

Table 3. Comparison between Total Energies and Energy Contributions Calculated for Optimized "Included" and "Excluded" Cobalt Cyclidene Adducts with 1-Methylimidazole

		E(total), kcal/mol	*E*(bond), kcal/mol	*E*(angle), kcal/mol	*E*(dihe), kcal/mol	*E*(vdW), kcal/mol	*E*(elec), kcal/mol
Co(unbr	included	−7.2	3.5	11.3	47.2	4.4	−74.3
Cyc)	excluded	−6.6	3.3	7.7	48.1	4.5	−71.1
(MeIm)	difference	−0.6	0.2	3.6	−0.9	−0.1	−3.2
Co(C3	included	51.1	12.1	37.1	67.0	13.6	−79.6
Cyc)	excluded	−7.0	3.1	8.0	55.8	1.0	−75.8
(MeIm)	difference	58.1	8.0	29.1	11.2	12.6	−3.8
Co(C6	included	19.9	6.9	25.4	56.0	9.0	−79.0
Cyc)	excluded	−5.5	4.1	11.1	48.6	5.9	−76.3
(MeIm)	difference	25.4	2.8	14.3	7.4	3.1	−2.7
Co(C8	included	2.5	4.9	16.5	54.3	4.6	−79.1
Cyc)	excluded	−3.6	4.7	12.3	48.7	5.9	−76.7
(MeIm)	difference	6.1	0.2	4.2	5.6	−1.3	−2.4
Co(C12	included	−4.2	4.7	14.9	49.5	2.4	−77.0
Cyc)	excluded	0.5	4.1	9.9	54.5	5.6	−75.2
(MeIm)	difference	−4.7	0.6	5.0	−5.0	−3.3	−1.8

simulation conditions corresponded to the isothermal−isobaric ensemble (with the internal pressure set to 1 atm and a temperature of 300 K), using Langevin dynamics on a pressure piston degree of freedom[47] and the Nose-Hoover algorithm[48,49] to control the temperature. A truncated octahedral cell[50,51] with periodic boundary conditions was used in all simulations of solvent-containing systems. In molecular dynamics simulations, SHAKE constraints[52] were imposed on bonds involving hydrogen atoms, providing a 2 fs time step.[53] The equations of motion were integrated by using a Verlet algorithm.[54] In energy calculations, a 12.0 Å nonbonded cutoff distance was employed with a switching function between 10.0 and 12.0 Å for van der Waals terms and a shift function at 12.0 Å for electrostatic terms to eliminate discontinuities due to the cutoff.[25]

The initial geometry of the included and excluded adducts Co(unbrCyc)(Meim) was taken from the optimized structures. The bond Co−N(MeIm) remained in the topology at the beginning of simulations. For both initial structures, the optimized molecule was placed in the center of a preequilibrated methanol cell (based on a cube of ca. 38 Å edge; the exact size of the cell depends on the linear dimensions of the particular complex and was selected in order to ensure that a solvent layer of at least 10 Å surrounds the macrocycle molecule within the primary cell). After deletion of the methanol molecules overlapping the solute, the included and excluded Co(unbrCyc)(Meim) systems contained 394 methanol molecules each. After brief energy minimization, heating, and 10 ps constant volume equilibration, the Co−N(MeIm) bond was deleted and the systems were allowed to evolve at constant pressure for 20 ps each followed by production runs at a constant pressure of 1 atm (200 ps for an included system and 160 ps for an excluded system). Coordinate sets were saved every 0.2 ps for subsequent analysis. The average temperature for both systems was 300 ± 6 K, and the average box size was 38.22 ± 0.16 and 38.24 ± 0.15 Å for included and excluded adducts, respectively.

Free Energy Simulations for the Included Co(unbrCyc)−MeIm System. The conformational free energy simulations were performed in the gas phase and in a methanol solvent box. The conformational free energy thermodynamic integration method developed by Kuczera[45,55] was used. Starting from the preequilibrated system with MeIm inside the cleft of Co(unbrCyc), a series of nine simulations were performed in which the value of the conformational coordinate (Co−N(MeIm) distance) was fixed consecutively at 2.0, 2.5, ..., 6.0 Å. The molecular dynamics protocol was identical to the one described above. Each free energy simulation consisted of a 20 ps equilibration and an 80 ps production run. In each case, the final structure from the trajectory with $r = r_0$ was used to start a simulation with $r = r_0 + 0.5$. Values of the free energy derivatives were stored every 0.04 ps and were used to calculate free energy derivatives with respect to the reaction coordinate in the postprocessing stage. Free energy profiles were calculated by integrating the corresponding derivatives.

Results and Discussion

Molecular Mechanics Calculations: Energy Minimization. Molecular mechanics calculations were performed to determine the degree of steric strain of the macrocycle upon inside-the-cavity axial ligand binding (included mode) compared to outside-the-cavity binding (excluded mode). For each macrocycle, five-coordinate adducts with 1-MeIm were optimized starting from the structures with the axial ligand included inside the cavity or bound outside the cavity. The binding mode of methylimidazole did not change after optimization, leading to two different optimized geometries (Figure 4). The energy difference between included and excluded five-coordinate adducts was used as a measure of steric interaction between the axial base and the walls and roof of the macrocyclic cleft. A direct comparison of the energies is possible in this case because the systems consist of the same atoms with the same covalent bonds. In molecular mechanics calculations, the absolute energies of different systems depend on the number and type of atoms included in the system. For this reason, the energies for the six-coordinate cobalt(II) cyclidenes having two axial bases cannot be directly compared to the energies for the corresponding five-coordinate complexes, where only one axial base is bound to the cobalt(II) ion.

The results for a series of bridged cyclidenes (Table 3) clearly demonstrate that the length of the polymethylene bridge is the critical parameter that determines the relative energy penalties for inside-the-cavity methylimidazole binding (included mode). In the case of a very short C3 bridge, the energy difference between included and excluded methylimidazole complexes is huge (greater than 50 kcal/mol), indicating that inside-the-cavity binding is impossible for this lacunar complex. The MeIm ligand is tilted and bent in the optimized included adduct, and the macrocycle is severely distorted (Figure 5a). Both cavity width

(47) Feller, S. E.; Zhang, Y. H.; Pastor, R. W.; Brooks, B. R. *J. Chem. Phys.* **1995**, *103*, 4613.
(48) Nose, S. *J. Phys. Chem.* **1984**, *81*, 511.
(49) Hoover, W. G. *Phys. Rev. A* **1985**, *31*, 1695.
(50) Adams, D. J. *Chem. Phys. Lett.* **1979**, *62*, 329.
(51) Allen, M. P.; Tildesley, D. J. *Computer Simulations of Liquids*; Clarendon: Oxford, 1987.
(52) Ryckaert, J. P.; Ciccotti, G.; Berendsen, H. J. C. *J. Comput. Phys.* **1977**, *23*, 327.
(53) Barth, E.; Kuczera, K.; Leimkuhler, B.; Skeel, R. D. *J. Comput. Chem.* **1995**, *16*, 1192.
(54) Verlet, L. *Phys. Rev.* **1967**, *159*, 98.
(55) Wang, Y.; Kuczera, K. *J. Phys. Chem. B* **1997**, *101*, 5205.

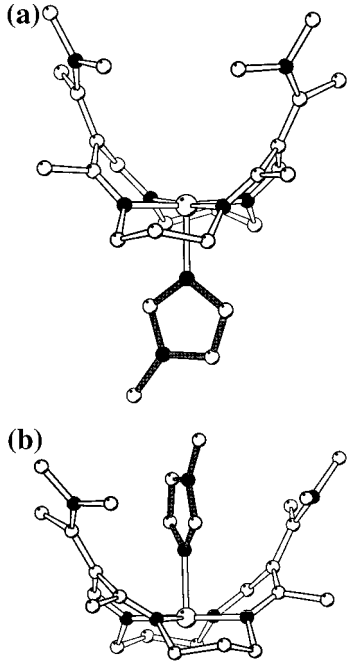

Figure 4. Optimized structures of five-coordinate 1-methylimidazole adducts with saddle-shaped unbridged cyclidene: (a) 1-methylimidazole located outside the cavity, excluded binding mode; (b) 1-methylimidazole located inside the cavity, included binding mode.

and cavity height are insufficient to accommodate the ligand within the cavity. The short C3 bridge is not flexible, so the "roof" of the cavity is rigid in this case. This bridge cannot flip away from the axial ligand binding site to provide more space for the incoming MeIm molecule. The short bridge also decreases the cavity width,[2,14,56] thus leading to additional constraints for the fifth ligand binding. As a result, the methylimidazole, if forced to be bound inside the cavity, interacts unfavorably with both the roof and the walls of the cavity and is pushed away from the ideal orientation with respect to the metal ion (perpendicular to the CoN_4 plane) (Figure 5a). All strain energy components corresponding to bonding interactions and nonbonded van der Waals energy increase substantially upon MeIm inclusion (Table 3). The computational results obtained here for the C3-bridged cyclidene are in complete agreement with the experimental data. It has been shown that even small molecules, such as O_2 or CO, cannot be bound to the metal ions inside the C3Cyc cavity.[56] As the bridge length increases, small molecule binding becomes possible and the O_2 binding constants reach a maximum value for the C8-bridged complex.[14] In the case of a larger ligand, MeIm, the inside-the-cavity binding appears to be unfavorable for C6-bridged cyclidene (Table 3), where a 25 kcal/mol energy penalty is still very significant to be considered a computational artifact. A primary source for this high energy of inclusion is the steric repulsion between the bridge and the incoming axial ligand (Figure 5b). The unbridged complex Co(unbrCyc), which is known to have approximately the same equilibrium cavity width as the Co(C6Cyc),[2,14,19] does not discriminate against the inside-the-cavity MeIm binding (Table 3). The unfavorable interactions between the included MeIm ligand and the bridge further decrease for the C8Cyc complex and completely disappear in the case of C12-bridged cyclidene (Table 3). While the C8 bridge flips away from the ligand binding site (similarly to the C6 bridge shown in Figure 5b), the C12 bridge is long enough

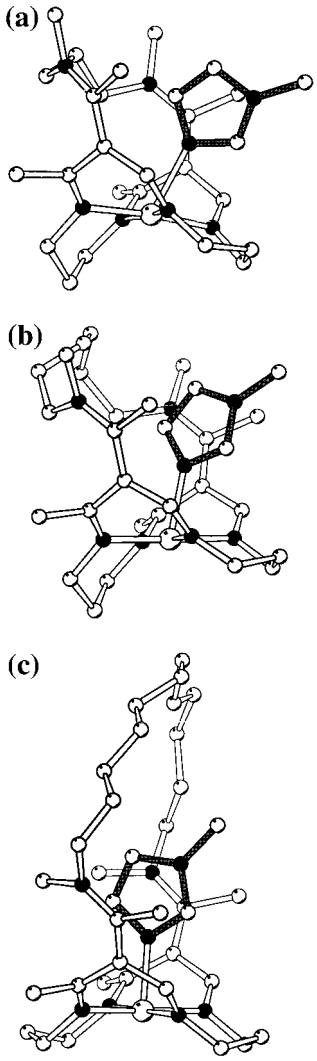

Figure 5. Optimized structures of bridged cobalt(II) cyclidenes with 1-methylimidazole bound inside the cavity: (a) C3-bridged complex; (b) C6-bridged complex; (c) C12-bridged complex.

to accommodate the incoming axial ligand underneath the "high roof" formed by the polymethylene chain (Figure 5c).

In the case of the unbridged saddle-shaped complex, Co(unbrCyc), the total energies calculated for the optimized included and excluded five-coordinate MeIm adducts are practically identical (Table 3): −7.2 and −6.6 kcal/mol, respectively. Although the macrocycle cavity width increases by 0.9 Å upon inside-the-cavity MeIm binding, the unfavorable strain energy of the macrocyclic ligand in the included MeIm adduct is compensated by the favorable nonbonded (electrostatic and van der Waals) interactions between the MeIm axial ligand and the cavity "walls". This result has been confirmed by molecular mechanics calculations on the two MeIm adducts (included and excluded), using a previously developed force field for cyclidenes based on MM2/MMP2 parameters.[26] The total energy of the optimized included adduct is equal to 14.4 kcal/mol, and the total energy of the corresponding excluded complex is 15.0 kcal/mol. The molecular mechanics calculations with two independently developed, different force fields (CHARM and MM2/MMP2) lead to the conclusion that the "walls" of the cavity alone, in the unbridged Co(unbrCyc), do not prevent the included MeIm binding mode. Therefore, the preferential existence of the five-coordinate instead of six-coordinate unbridged complexes in solutions should be caused by electronic, rather than steric, factors.

(56) Herron, N.; Chavan, M. Y.; Busch, D. H. *J. Chem. Soc., Dalton Trans.* **1984**, 1491.

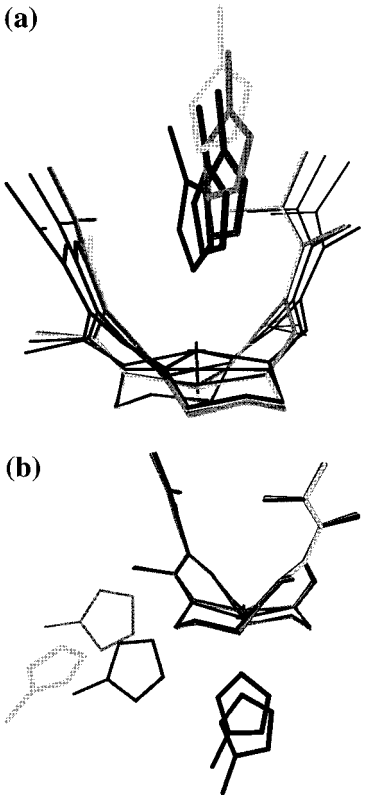

Figure 6. Series of optimized structures for a two-fragment system consisting of Co(unbrCyc) and 1-MeIm, with Co−N(MeIm) distance fixed at 2.00, 3.00, 4.00, 5.00, and 6.00 Å: (a) included MeIm binding mode (the ligand approached the cobalt(II) center from inside the cavity); (b) excluded MeIm binding mode (the ligand approached the Co(II) center from outside the cavity).

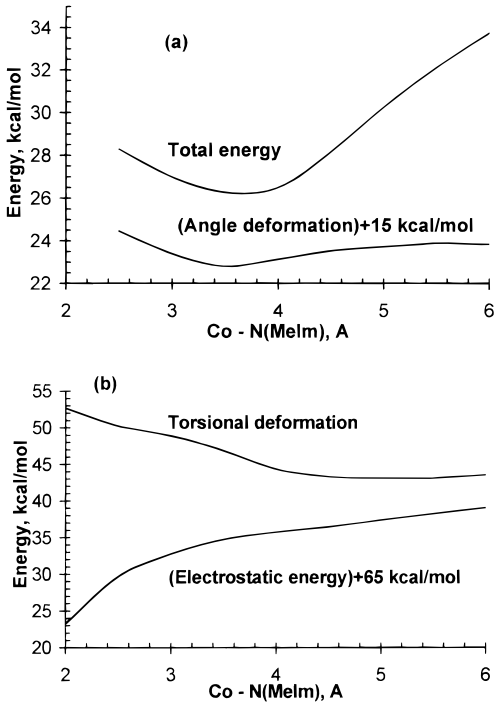

Figure 7. Adiabatic energy profile for 1-methylimidazole approaching cobalt(II) metal ion in Co(unbrCyc) from inside the cavity: (a) total energy changes along the Co−N(MeIm) coordinate, and energy of angle deformations; (b) contributions from electrostatic interactions and torsional deformational energy.

Molecular Mechanics Calculations: Adiabatic Energy Profile for Methylimidazole Translation. Further insights into the possible differences between included and excluded complexation of MeIm with saddle-shaped unbridged cyclidenes could be gained from the analysis of the ligand−complex interactions along the Co−N(MeIm) reaction coordinate. To evaluate the geometry and energy changes along the pathway for MeIm entering the cavity of the unbridged cyclidene, the constrained molecular mechanics calculations have been performed. The Co−N(MeIm) bond and the corresponding angle and dihedral terms were deleted from the topology file. Instead, as parts of two separate molecular fragments, the Co and N(MeIm) atoms experienced standard nonbonded interactions and a holonomic constraint was imposed to hold the Co··· N(MeIm) distance at a fixed value. These calculations were complemented with free energy simulations discussed below.

The optimized geometry of the Co(unbrCyc)(MeIm) adduct (either included or excluded) was used as a starting point in the constrained molecular mechanics calculations. The fixed Co−N(MeIm) distance was incrementally increased from 2 to 6 Å in 0.5 Å steps. All other positional parameters associated with methylimidazole ligand were not constrained in any manner. It was found that the included MeIm molecule remains perpendicular to the $Co(N_4)$ plane and moves along the normal to this plane (Figure 6a). Even at a distance of 6 Å, the orientation of the MeIm molecule with respect to the $Co(N_4)$ plane is almost identical with its orientation in the vicinity of the cobalt ion (Figure 6a). The same results are obtained when MeIm was originally placed 6 Å apart from the Co(II) ion, with the Co−N(MeIm) axis orthogonal to the $Co(N_4)$ plane. In this case, MeIm was translated by 0.5 Å toward the Co(II) ion along the Co−N(MeIm) axis, and the new structure was optimized. The procedure was repeated until the Co−N(MeIm) distance reached 2 Å. While the orientation of MeIm does not change significantly upon its translation toward the metal center, because the pathway into the cavity is restricted by the "walls" of the unbridged macrocycle, the geometry of the macrocycle itself changed in order to accommodate the incoming MeIm molecule (Figure 6a). As MeIm approaches the Co(II) ion, the cavity opens up (by ca. 0.9 Å) and the Co(II) ion moves toward the incoming MeIm ligand (by ca. 0.3 Å).

In contrast, when MeIm is translated away from the Co(II) ion in the excluded adduct, the ligand orientation is preserved only up to a Co−N(MeIm) distance of 3.5 Å. At greater distances from the metal ion, the MeIm orientation is not restricted (Figure 6b). Moreover, when the calculations are performed in a "reversed" order, starting with a configuration with a MeIm molecule orthogonal to the $Co(N_4)$ plane and placed at 6 Å from the Co(II) center, the axial ligand moves away from this normal plane in an optimized structure (Figure 6b). At a distance of 3.5 Å, MeIm spontaneously moves in the plane orthogonal to the $Co(N_4)$ plane. The axial ligand remains in this plane, typical of the bound MeIm, until it approaches Co(II) at a distance of 2 Å. Since there is no obvious steric interaction between the excluded MeIm molecule and the saddle-shaped unbridged cyclidene, the conformation of the macrocycle does not change substantially upon MeIm translation to (or away from) the metal ion (Figure 6b).

Energy profiles along the MeIm translation pathways are also different for the two initial ligand positions (included and excluded). For the excluded coordination mode, the total energy drops dramatically from 2 to 2.5 Å and then slowly and monotonically increases at larger Co−N(MeIm) distances (Figure 7a). A somewhat artificial increase in energy at a short distance is due to a van der Waals contribution, which arises because of the absence of the explicit Co−N(MeIm) bond in

the topology file. As a result, the molecular mechanics algorithm does not consider the Co atom and the N(MeIm) atom as being connected by a chemical bond even at a short distance of 2.0 Å and the van der Waals repulsive energy between these two atoms is calculated as one of the nonbonded interactions. An increase in the total energy at larger Co−N(MeIm) distances is related to a decrease in a favorable electrostatic contribution (Figure 7).

For an included adduct, the analysis of the total energy change along the Co−N(MeIm) coordinate shows no barrier for MeIm to enter the cleft. Furthermore, a shallow but distinct energy minimum is present at a distance of 3.5 Å. The origin for this minimum can be found from an analysis of individual energy components. The bond, angle, and van der Waals energy components experience minor changes upon MeIm translation (an increase in van der Waals energy at 2 Å can be discounted, as discussed above). It should be noted that the angle term is changing in parallel with the total energy at short distances (up to 3.5 Å), so it does contribute to the total energy profile in this conformational region (Figure 7a). The most significant changes are seen in dihedral and electrostatic terms (Figure 7b). As expected, the dihedral energy decreases substantially with an increase in Co−N(MeIm) distance (from 53 kcal/mol at 2 Å to 45 kcal/mol at 4 Å, and then it remains almost unchanged). At the same time, the electrostatic energy increases from −42 kcal/mol at 2 Å to −31 kcal/mol at 4 Å, with a further increase to −26 kcal/mol at 6 Å. An interplay between the macrocyclic strain energy, as reflected in angle and dihedral energy terms (unfavorable at short distances between the cobalt atom and the included ligand), and the nonbonded electrostatic energy (more favorable at short distances and less favorable at long distances between the cobalt atom and the included ligand) results in a total energy curve with a minimum at about 3.5 Å. This minimum on the total energy curve corresponds to the presence of a weak MeIm binding site, which is located at the entrance of the macrocyclic cavity.

Molecular mechanics calculations reveal the absence of an energy barrier for MeIm to enter the cleft of the unbridged shaddle-shaped cyclidene, and the presence of a weak MeIm binding site at the entrance of the cavity. These calculations are particularly useful for analysis of individual contributions of the energy components to the total energy. The molecular mechanics does not, however, provide any information on the dynamic behavior of the system Co(unbrCyc)−MeIm nor does it allow for evaluation of the solvation effects. The free energy profile for MeIm translation to/from the Co(II) center, which includes both enthalpic and entropic contributions, is also desirable for the description of interactions in the system. To obtain these data, molecular dynamics simulations were performed.

Molecular Dynamics Simulations for Included and Excluded Co(unbrCyc)−MeIm Systems in Methanol. For each system (included or excluded), the optimized structure obtained in unconstrained molecular mechanics calculations was used as the initial geometry of an adduct. The five-coordinate complex Co(unbrCyc)(MeIm) was placed in the middle of a preequilibrated methanol solvent box. The methanol molecules overlapping with the solute were deleted, and the system was then equilibrated at 300 K for 20 ps using constant volume simulation conditions. After the equilibration was complete, the Co−N(MeIm) bond (and corresponding angles and dihedrals) was deleted and the system was allowed to evolve, under constant pressure (1 atm) simulation conditions, for 220 ps (included system) or 180 ps (excluded system). The first 20 ps of these simulations were discarded from the production runs.

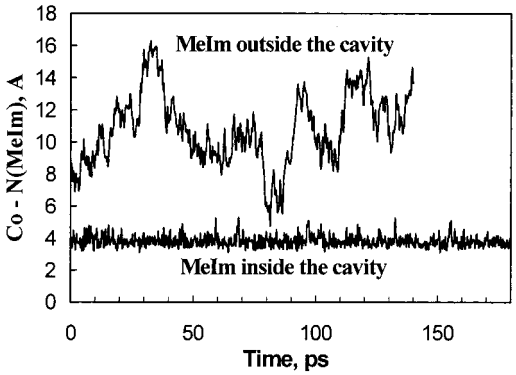

Figure 8. Time evolution of the Co−N(MeIm) distance in the course of molecular dynamics simulations for a two-fragment system consisting of the Co(unbrCyc) complex and the MeIm ligand: included initial geometry (solid line) vs excluded initial geometry (dotted line).

The included and excluded isomers demonstrated distinctly different behavior in the course of the simulation. After the Co−N(MeIm) bond was destroyed, the axial ligand initially bound from outside the cavity diffused freely in the solvent box (Figures 8 and 9). The Co−N(MeIm) distance during the production run falls within a broad range between 5 and 17 Å, with an average of 10.8 Å and root-mean-square fluctuations of 2.2 Å (Figure 8). At no time did the MeIm molecule approach the Co(II) center in the macrocycle, and the base and the macrocycle behaved as two independent species in the simulations.

In contrast, in the case of the included isomer, the absence of the explicit Co−N(MeIm) bond did not lead to free diffusion of the MeIm molecule into the bulk of the solvent. After the Co−N(MeIm) bond was deleted, the axial ligand quickly moved to ca. 4 Å from the Co(II) ion and stayed at this distance for the whole 200 ps simulation (at an average Co−N distance of 3.83 Å, with rms fluctiations of 0.25 Å) (Figures 8 and 10). The location of the methylimidazole at the entrance of the cavity corresponds approximately to the total energy minimum obtained in constrained molecular mechanics calculations. Therefore, even without an explicit bond between Co(II) and N(MeIm) atoms, the originally included methylimidazole molecule does not leave the macrocyclic cleft within 200 ps of the simulations.

The conformation of the macrocycle did not change significantly during the simulations for either included or excluded initial geometries of the five-coordinate adducts Co(unbrCyc)(MeIm) (Figures 9 and 10). Moreover, the macrocycle cleft width was remarkably similar in both simulations. The average distance between atoms C3 and C19 was 4.85 ± 0.15 and 4.83 ± 0.16 Å, the distance C39−C40 was equal to 5.95 ± 0.25 and 5.93 ± 0.25 Å, and the N45−N58 distance was 5.72 ± 0.27 and 5.69 ± 0.25 Å for included and excluded adducts, respectively. These data indicate that the presence of an axial ligand at the entrance of the cleft, at a relatively large distance from the central metal ion, does not cause any distortion of the saddle-shaped cyclidene geometry in a solvated system. It appears that there are no close van der Waals contacts between the methylimidazole molecule located at this weak noncovalent binding site and the walls of the cyclidene molecule (Figure 9). This conclusion is supported by the results of constrained molecular mechanics calculations on two-fragment systems (see previous section and Figure 6); significant changes in macrocycle geometry upon MeIm inclusion have been observed at short Co−N(MeIm) distances (less than 4 Å), while at Co−N(MeIm) distances greater than 4 Å the macrocycle cavity width remained almost unchanged. Solvation effects in our molecular dynamics simulations are also important for leveling off the

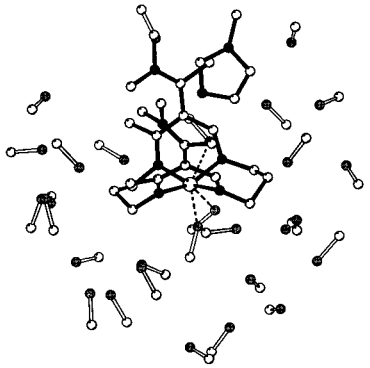

Figure 9. Trajectory snapshot from molecular dynamics simulation in methanol for a two-fragment system Co(unbrCyc)−MeIm (no explicit Co−N(MeIm) bond), with included MeIm initial geometry. 1-Methylimidazole remains in the vicinity of the cyclidene cleft.

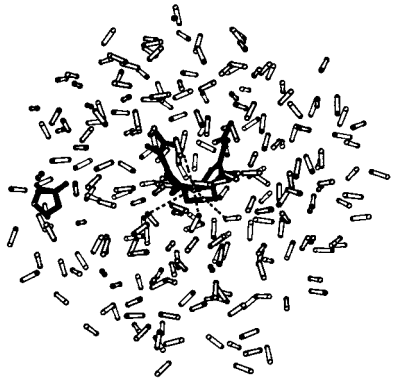

Figure 10. Trajectory snapshot from molecular dynamics simulation in methanol for a two-fragment system Co(unbrCyc)−MeIm (no explicit Co−N(MeIm) bond), with excluded MeIm initial geometry. 1-Methylimidazole freely diffuses in the solvent box.

macrocyclic cavity width in both included and excluded MeIm adducts. A weak noncovalent ligand binding site located at the entrance of the cyclidene cavity is occupied by MeIm in the included adduct and is occupied by a solvent (methanol) molecule in the excluded complex (Figure 6). Solvation of the sides of the unbridged saddle-shaped cyclidene complex has been demonstrated previously.[22] van der Waals repulsion, if any, between the walls of the cyclidene and either MeOH or MeIm molecule bound at the periphery of the cleft should be very similar, leading to practically identical macrocycle conformations in solvated excluded and included two-fragment systems.

While the difference in trajectories of initially included and excluded MeIm adducts is revealing in terms of confirming the presence of a binding site at the entrance of the cleft, it also indicates an insufficient sampling of the conformational space, at least in the case of the included complex. Indeed, the topology of the included and excluded adduct is identical, and in the absence of the Co−N(MeIm) bond, the trajectories started from two different initial geometries should eventually converge. The observation that the initially included methylimidazole does not visit the areas in the solvent box remote from the macrocyclic cleft indicates that the free energy profile for MeIm translation cannot be obtained by a direct sampling method. To accomplish more efficient sampling of the conformational space, a conformational free energy simulation protocol was used.

Conformational Free Energy Simulations: Free Energy Profile for MeIm Entering the Macrocyclic Cleft. The free energy simulations were performed for an included initial geometry of a Co(unbrCyc)(MeIm) complex. The Co−N(MeIm) bond was deleted, and the distance between the Co(II) ion and the nitrogen from MeIm was used as a conformational coordinate. A series of simulations were performed, with the Co−N(MeIm) distance constrained to a particular value (in the range from 2 to 6 Å). The thermodynamic integration method described in refs 45 and 55 was used in the conformational free energy analysis. The potential of mean force along the Co−N(MeIm) coordinate was obtained for both vacuum and solution (methanol) simulations. The derivative (dw/dr) of the potential of mean force w with respect to the distance r was calculated directly and then integrated numerically to give the $w(r)$ dependence.

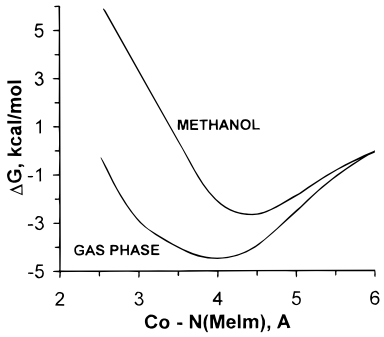

Figure 11. Results of the conformational free energy simulations for an included MeIm adduct with Co(unbrCyc). The potential of mean force has been calculated in the simulations and transformed into the free energy profile using eq 1.

The physical meaning of the potential of mean force is that $w(r_2) - w(r_1)$ represents the reversible work of changing the system from a state with $r = r_1$ to a state with $r = r_2$. In principle, there is a difference between $w(r)$ and the conformational free energy $G(r)$, which is related to the probability of finding a system with a reaction coordinate equal to r. This difference involves a thermodynamic average of a volume element (Jacobian) describing the transformation linking the atomic Cartesian coordinates and the reaction coordinate.[45] This correction was not calculated directly but was estimated by the known result for the case of the $w(r)$ of two spherically symmetric atoms:

$$G(r) = w(r) - kT \ln r^2 + \text{const} \qquad (1)$$

where the constant is set so that $G(r) = 0$ at a chosen point. This form of the correction is only approximate for our system, where some effects from the sterically excluded volume may be expected. In practice the actual values of the correction term were quite small and were neglected for the purpose of the following discussion.

The free energy profiles for MeIm entering the cleft of the unbridged Co(II) cyclidene (Figure 11) are qualitatively similar to the adiabatic profile obtained in constrained molecular mechanics calculations. A relatively shallow minimum at a Co−N(MeIm) distance of about 4 Å indicates the presence of a weak MeIm binding site at the entrance of the macrocyclic cleft. Quantitative differences can be seen in the exact location of the minimum and in the depth of the energy minimum. In the case of gas-phase simulation, the free energy minimum is relatively deep (4 kcal/mol) and is located at a somewhat shorter Co−N(MeIm) distance (3.5 Å) than the free energy minimum obtained in a solution simulation (a depth of ca. 2 kcal/mol and a Co−N distance of 4 Å). This difference should be attributed to solvation effects. In methanol, both the methylimidazole and the macrocycle are solvated. A number of solvent−solute interactions are broken when MeIm leaves the bulk solvent and

enters the cavity of the saddle-shaped complex. As a result, the free energy difference between MeIm in a bulk solvent (as approximated by MeIm located 6 Å apart from the cobalt atom) and included MeIm decreases (a favorable interaction with the macrocycle is partially compensated by an unfavorable desolvation energy). It is also clear that in the solvent box, the free energy minimum is shifted farther apart from the metal ion. This remote position of the incoming ligand allows for its better solvation. Enthalpy−entropy decomposition of the free energy might be useful in providing more insight into the nature of the weak MeIm binding at the entrance of the macrocycle. An attempt to calculate the enthalpy and entropy contributions separately, however, did not appear to yield reliable data because the fluctuations (and statistical errors) in enthalpic and, especially, entropic contributions were too high.

Comparison with Experimental Data. The computational results detailed above focused on steric aspects of methylimidazole binding inside the clefts of constrained cobalt(II) cyclidenes. It is desirable to increase the generality of our approach, addressing directly (a) the role of electronic factors in small ligand binding to cyclidene complexes, (b) the binding of a broad range of axial ligands other than methylimidazole, and (c) ligand binding to square-planar sterically hindered complexes of other metal ions. Several different approaches to these problems are viable. One of them is to perform detailed electronic structure calculations (ab initio or DFT) on each system of interest. While this approach is expected to provide the most accurate information on the electronic structure and energetics of ligand binding, it is still computationally very expensive. Moreover, any modifications in the system (e.g., changes in the macrocycle structure, variations in the central metal ion, or replacement of the axial ligand) require repetition of the calculations. The applications of quantum chemistry calculations to a broad range of similar systems are thus limited, and the calculations were not attempted in the current work. Another approach is to utilize the force field developed here for MM/MD calculations on relevant chemical systems. Using this approach, we were able to reproduce experimental trends in O_2/CO affinities of iron(II) cyclidenes.[57] Finally, comparing our computational results on MeIm binding to Co(II) cyclidenes with the available experimental data obtained for similar metallohosts and guests allows for better understanding and better prediction of the binding affinities of the hosts. The steric requirements of metal-containing platforms are primarily determined by the structure of the macrocyclic ligands, while their electronic structure is a function of a particular metal ion.

The behavior of a d^7 Co(II) ion with respect to axial ligand binding is somewhat different from that of d^6 ions, such as Co(III) or Fe(II). Macrocyclic ligands, especially those with several double bonds in the ring, tend to be strong field ligands and form low-spin cobalt(II) complexes.[2,58,59] In the idealized octahedral geometry, e_g orbitals are doubly degenerate and decompose into two spatial orbitals, one axial (d_{z^2}) and one equatorial ($d_{x^2-y^2}$). A strong equatorial ligand field causes destabilization of a d_{z^2} orbital of a low-spin d^7 cobalt(II) ion, which decreases significantly the affinity for axial ligand binding (in particular, six-coordinate adducts become destabilized). In contrast, the electrons of low-spin Co(III) or Fe(II), d^6, fill the t_{2g} obitals, making a stable six-coordinate octahedral geometry with no low-lying vacant orbitals. It appears that the electronic configuration of the metal ion affects the degree of distortion of the local environment within the metal coordination sphere (donor atoms) but not the conformation of the macrocycle. For example, the C6Cyc conformations in Co(II) and Co(III) complexes are practically indistinguishable (saddle-shaped in both cases).[2,14,16]

Low-spin Co(II) complexes with tetradentate ligands may preferentially exist in solutions in the presence of additional monodentate ligands (solvent or base molecules) in the form of four-, five-, or six-coordinate species. The electron spin resonance (ESR) technique is very useful for distinguishing between complexes having one or two axial nitrogen donor ligands because the superhyperfine splitting is different for these two types of complexes. A three-line splitting pattern is observed in the spectra of five-coordinate complexes, while five lines are characteristic for the six-coordinate species.[59]

Cobalt(II) complexes with sterically nonhindered tetradentate ligands tend to bind additional axial base molecules (usually one, but sometimes two). For example, the ESR spectra of planar cobalt(II) BF_2-substituted dimethylglyoxime complexes in acetonitrile solution with excess pyridine showed that the nitrogenous axial base ligands produce three or five superhyperfine lines.[60] This indicates that either one or two axial base molecules may bind to the cobalt. Similar results have been obtained for low-spin Co(II) complexes with Schiff bases derived from salicylaldehyde, acetylacetone, or related β-diketones.[61−64] In the case of Co(II) porphyrins, five-coordinate species usually dominate in solutions, but six-coordinate adducts can be obtained at high concentrations of axial bases.[65−67] Interestingly, pyridine derivatives form six-coordinate complexes with cobalt(II) porphyrins relatively easily, while imidazole derivatives preferentially form five-coordinate adducts.[66,67]

The ESR spectra of the unbridged complex [Co(unbrCyc)]-$(PF_6)_2$ in acetonitrile solution are consistent with typical five-coordinate, low-spin d^7 structures having tetragonal pyramidal geometries, both in the absence and in the presence of a strong axial base, 1-methylimidazole.[15,20] Such behavior is parallel to that of lacunar cobalt(II) cyclidenes, which are known to coordinate only one molecule of a solvent (e.g., acetonitrile) or base (e.g., methylimidazole).[2,14]

The preferential formation of five-coordinate cobalt(II) cyclidene complexes in solutions containing pyridine or imidazole derivatives as axial bases also follows from our previous studies of the kinetics of dioxygen binding.[17,68] The oxygenation of Co(II) cyclydenes is a fast, low-barrier process with negative activation entropies, which is consistent with Co(II)−O_2 bond formation (a process similar to radical combination) but not with the dissociation of the sixth ligand (solvent or base) from the Co(II) center.[17,68] The kinetic parameters do not change with an increase in the methylimidazole concentration from 0.1 to 1.5 M. These findings suggest that Co(II) 16-membered cyclidenes (both unbridged and bridged) coordinate only one

(57) Buchalova, M.; Rybak-Akimova, E. V.; Kuczera, K.; Busch, D. H. Manuscript in preparation.
(58) Lindoy, L. F. *The chemistry of macrocyclic ligand complexes*; Cambridge University Press: Cambridge, 1989.
(59) Smith, T. D.; Pilbrow, J. R. *Coord. Chem. Rev.* **1981**, *39*, 295.
(60) Lance, K. A.; Goldsby, K.; Busch, D. H. *Inorg. Chem.* **1990**, *29*, 4537.
(61) Hoffman, B. M.; Diemente, D. L.; Basolo, F. *J. Am. Chem. Soc.* **1970**, *92*, 61.
(62) Carter, M. J.; Rillema, D. P.; Basolo, F. *J. Am. Chem. Soc.* **1974**, *96*, 393.
(63) Kubokura, K.; Okawa, H.; Kida, S. *Bull. Chem. Soc. Jpn.* **1978**, *51*, 2036.
(64) Chen, Y.-Y.; Chu, D. E.; McKinney, B. D.; Willis, L. J.; Cummings, S. C. *Inorg. Chem.* **1981**, *20*, 3582.
(65) Stynes, D. V.; Stynes, H. C.; James, B. R.; Ibers, J. A. *J. Am. Chem. Soc.* **1973**, *95*, 1796.
(66) Walker, F. A. *J. Am. Chem. Soc.* **1973**, *95*, 1154.
(67) Walker, F. A. *J. Am. Chem. Soc.* **1970**, *92*, 4235.
(68) Rybak-Akimova, E. V.; Masarwa, M.; Marek, K.; Warburton, P. R.; Busch, D. H. *Chem. Commun.* **1996**, 1451−1452.

methylimidazole molecule in solutions (acetone, acetonitrile, or methanol was used as solvent).[17,68]

Electrochemical studies also supported the presence of a five-coordinate Co(II) species, while Co(III) compounds appear to be six-coordinate. An irreversible electrochemical behavior for the unbridged complex $[Co(unbrCyc)](PF_6)_2$ has been reported for the Co^{III}/Co^{II} redox couple.[20,69] This irreversible electrochemical phenomenon suggests that the coordination number changes from five to six when the Co(II) species is oxidized to the Co(III) species. The electrochemical studies of the lacunar cobalt(II) cyclidene complexes[69] indicate that the 2+/3+ redox couple of the short-bridged cobalt complexes (C3, C4, and C5-bridged) is reversible in both acetonitrile and acetone solution. The lacunar cobalt complexes with long bridges (C6, C7, and C8) and, consequently, larger cavities show quasi-reversible behavior in acetonitrile solution and reversible behavior in acetone solution, wherein the poor Lewis base, acetone, may not bind to the cobalt. These data show that Co(III) cyclidenes with long enough bridges (C6 or longer), unlike Co(II) cyclidenes, can bind the solvent molecules within the cavity.[69]

It can be concluded from the available experimental data that the Co(II) complexes with cyclidene ligands coordinate only one axial base molecule and do not form six-coordinate adducts. This remains true for bridged cyclidenes with different bridge length and for unbridged cyclidenes. Our computational results indicate that there is no steric hindrance associated with inside-the-cavity MeIm binding to the unbridged and C12-bridged cyclidenes. Consequently, preferential formation of five-coordinate Co(II) complexes in these cases is caused by electronic factors. For the bridged cyclidenes with the short bridges, both electronic and steric factors favor five-coordinate Co^{II}(Cyc)(MeIm) adducts. Our results on methylimidazole binding to the saddle-shaped unbridged Co(II) cyclidene, in combination with the experimental data for this system, allow for the following predictions: (1) Co(II) complexes with planar 14-membered unbridged cyclidenes will still bind only one axial ligand; (2) Co(III) or Fe(II) complexes with the saddle-shaped 16-membered unbridged cyclidene should be able to coordinate two methylimidazole molecules; (3) Co(III) or Fe(II) complexes with the saddle-shaped 16-membered cyclidene will bind only one bulky axial base because of steric protection of the walls of the cleft; (4) Co(III) or Fe(II) complexes with bridged cyclidenes will bind the flat aromatic axial ligands inside the cavity and form six-coordinate complexes if the bridge is long enough. Statements 1−3 can be tested experimentally; statement 4 is in agreement with the experimental data for Co(III) and Fe(II) cyclidene complexes.[21,70,71] Indeed, electrochemical data discussed above show that Co(III) cyclidenes form six-coordinate adducts.[69] Some of them (with SCN^- ligand) were structurally characterized.[2,16,72] The behavior of iron(II) cyclidenes with respect to the sixth ligand binding parallels that of Co(III) complexes. While Fe(II) complexes with C4 and C5 cyclidenes exist in solutions (in acetone−pyridine−water or acetonitrile−1-methylimidazole solvent systems) as high-spin, five-coordinate species, the complex with C6 cyclidene displays a distinct spin equilibrium, which is shifted toward the formation of six-coordinate complexes at low temperature (−40 °C),[21,70,71] and $Fe(C8Cyc)^{2+}$ has a significant fraction of a six-coordinate complex even at room temperature.[57] Thus, the complexes of d^6 ions (Co(III) and Fe(II)) bind the coordinating solvent molecules in the sixth position unless the short bridges (C4 or C5) sterically protect the sixth metal site. The available data did not allow for distinction between a small solvent molecule or a bulkier base molecule binding at the sixth metal coordination site. These results are in quantitative agreement with our molecular mechanics calculations (Table 3).

Conformational free energy simulations indicate the presence of a weak MeIm binding site at the cavity entrance. This result can also be tested experimentally and is in agreement with the data on similar systems. Although we are unaware of direct experimental observations of an axial base trapped at the entrance of the cyclidene cavity, the structural data on cyclidene adducts with benzonitrile or acetonitrile show the polar guests located near the entrance of the cavity, with the nitrogen atom pointing to the metal ion.[73,74] NMR relaxation methods can be used to determine experimentally the position of weakly bound methylimidazole with respect to a paramagnetic central metal ion. Similar experiments proved to be extremely informative in mapping hydrophobic guest binding within the hydrophobic cavities of superstructured vaulted cyclidenes.[73,75−77]

Conclusions

Detailed molecular modeling studies demonstrate that the "walls" of the cleft create some steric hindrance around the sixth binding site but not for the binding of flat aromatic bases (1-methylimidazole was used in our studies). In the case of Co(II) unbridged cyclidenes, electronic factors should be responsible for the formation of five-coordinate adducts with the bases. For other metal ions with preferable six-coordinated octahedral geometry, the sixth ligand binding can be prevented by steric interactions between the incoming ligand and the "roof" of the cyclidene. Molecular dynamics and free energy simulations reveal the presence of a weak methylimidazole binding site at the entrance of the cleft of Co(unbrCyc).

Acknowledgment. The authors gratefully acknowledge the University of Kansas Molecular Modeling and Graphics Laboratory and Kansas Institute for Theoretical and Computational Science for making available their computer resources for a part of this project. We thank Prof. D. H. Busch for helpful discussions, Prof. N. W. Alcock for providing the X-ray coordinates for several cyclidene complexes in a computer readable format, Prof. K. B. Lipkowitz for providing topology and parameter files for cobalt macrocyclic complexes, and Dr. A. Hermone for providing the CHARMM force field parameter file for retinal. We are grateful to the referees for helpful suggestions.

Supporting Information Available: figure showing complete atom numbering schemes, and CHARMM topology and force field parameter listings. This material is available free of charge via the Internet at http://pubs.acs.org.

IC990738L

(69) Chavan, M. Y.; Meade, T. J.; Busch, D. H.; Kuwana, T. *Inorg. Chem.* **1986**, *25*, 314.
(70) Dickerson, L. D.; Sauer-Masarwa, A.; Herron, N.; Fendrick, C. M.; Busch, D. H. *J. Am. Chem. Soc.* **1993**, *115*, 3623.
(71) Buchalova, M.; Warburton, P. A.; van Eldik, R.; Busch, D. H. *J. Am. Chem. Soc.* **1997**, *119*, 5867.
(72) Jackson, P. J.; Cairns, C.; Lin, W.-K.; Alcock, N. W.; Busch, D. H. *Inorg. Chem.* **1986**, *25*, 4015.
(73) Meade, T. J.; Alcock, N. W.; Busch, D. H. *Inorg. Chem.* **1990**, *29*, 3766.
(74) Takeuchi, K. J.; Busch, D. H.; Alcock, N. W. *J. Am. Chem. Soc.* **1983**, *105*, 4261.
(75) Kwik, W.-L.; Herron, N.; Takeuchi, K. J.; Busch, D. H. *J. Chem. Soc., Chem. Commun.* **1983**, 409.
(76) Meade, T. J.; Kwik, W.-L.; Herron, N.; Alcock, N. W.; Busch, D. H. *J. Am. Chem. Soc.* **1986**, *108*, 1954.
(77) Meade, T. J.; Takeuchi, K. J.; Busch, D. H. *J. Am. Chem. Soc.* **1987**, *109*, 725.